Analysis of supplementary information emerging from the ICA based ICTD

Nikola Besic, Gabriel Vasile, Jocelyn Chanussot, Srdjan Stankovic, Alexandre Girard, Guy d'Urso

ANALYSIS OF SUPPLEMENTARY INFORMATION EMERGING FROM THE ICA BASED ICTD

N. Besic[1,2], G. Vasile[1], J. Chanussot[1,3], S. Stankovic[2], A. Girard[4] and G. d'Urso[4]

[1] GIPSA-lab, Grenoble-INP/CNRS, Grenoble, France, nikola.besic@gipsa-lab.grenoble-inp.fr
[2] Faculty of Electrical Engineering, University of Montenegro, Podgorica, Montenegro
[3] Faculty of Electrical and Computer Engineering, University of Iceland, Reykjavik, Iceland
[4] R&D STEP, Electricity of France (EDF), Chatou, France

ABSTRACT

This paper presents an elaboration of the ICA based ICTD, proposed in [1]. The method is applied on three different datasets and three distinctive aspects of its performances are considered. Firstly, we challenge the initial choice of the ICA algorithm, by testing the suitability of two representative tensorial (fourth-order) and one second-order algorithm. Further, we demonstrate the invariance of the proposed decomposition with respect to both the rotation around the line of sight and the change of polarisation basis. Finally, we analyse the potential of supplementary information contained in the second most dominant component.

Index Terms— ICA, ICDT, invariance, distributed targets

1. INTRODUCTION

Two essentially used algebraic Incoherent Target Decomposition (ICTD) methods: the H/α decomposition [2] and the Touzi decomposition [3], are both relying on the eigenvector decomposition (EVD) of the target coherence (or covariance) matrix. Under certain constraints, the EVD can be considered equivalent to the Principal Component Analysis (PCA). Thus, strictly speaking, the conventional ICTD methods result in deriving statistically independent components only in case of a Gaussian homogeneous POLSAR clutter. On the other side, given the improvement in spatial resolution, the POLSAR data are rather characterized by Non-Gaussian heterogeneous clutter [4], in which case the conventionally derived components are uncorrelated but not statistically independent. Therefore, in order to derive independent components by exploiting higher order statistical moment, in [1, 5] we presented an alternative approach dedicated to the analysis of very-high resolution POLSAR images, by introducing the Independent Component Analysis (ICA) instead of the EVD.

In this article, we elaborate the proposed ICA based ICTD, by applying it on three different datasets and by considering three different aspects of its performances.

This work was supported by the French National R&DProgram TSEN-X PEPS UJF-CNRS 2013.

First of all, we challenge the initial choice of the Complex NC FastICA algorithm [6], by observing, in the context of the ICTD, suitability of the most representative tensorial methods [7] and one second order method. After employing the Forth-Order Blind Identification (FOBI) [8], the Joint Approximate Diagonalization of Eigenmatrices (JADE) [9] and the Second-Order Blind Identification (SOBI) [10] in deriving independent backscattering mechanisms, we compare the estimated entropy and Target Scattering Vector Model (TSVM) parameters with their counterparts emerging from classical (PCA based) method. Although the FOBI exhibits some interesting properties, the initial choice seems to be justified.

As well, we demonstrate the invariance of the ICA based ICTD under the rotation of the line of sight and under the change of polarization basis. For the latter we use the projection of the observations onto the circular polarization basis, coupled with the Circular Polarization Scattering Vector (CPSV) model [11].

Finally, we analyse the potential of supplementary information contained in the second most dominant component of the proposed ICTD method, based on the ICA [1]. The method is applied on two POLSAR ALOS L-band images, where the helicity of the second most dominant component allows a discrimination between the classes corresponding to dry snow, wet snow and bare ground.

2. THE ICA BASED ICDT

The method [5] principally consists of three steps. The first step assumes the selection of the observation data. This is done either globally (statistical classification, e.g. [12]), or locally (sliding window). Further, we apply the ICA algorithm on the selected set of target vectors, obtaining a mixing matrix and corresponding sources. The columns of the estimated mixing matrix are the target vectors of the independent backscattering mechanisms, while their squared ℓ_2 norms define the contribution to the total backscattering. The third step is the parametrization of the obtained target vectors, done by means of the TSVM [3].

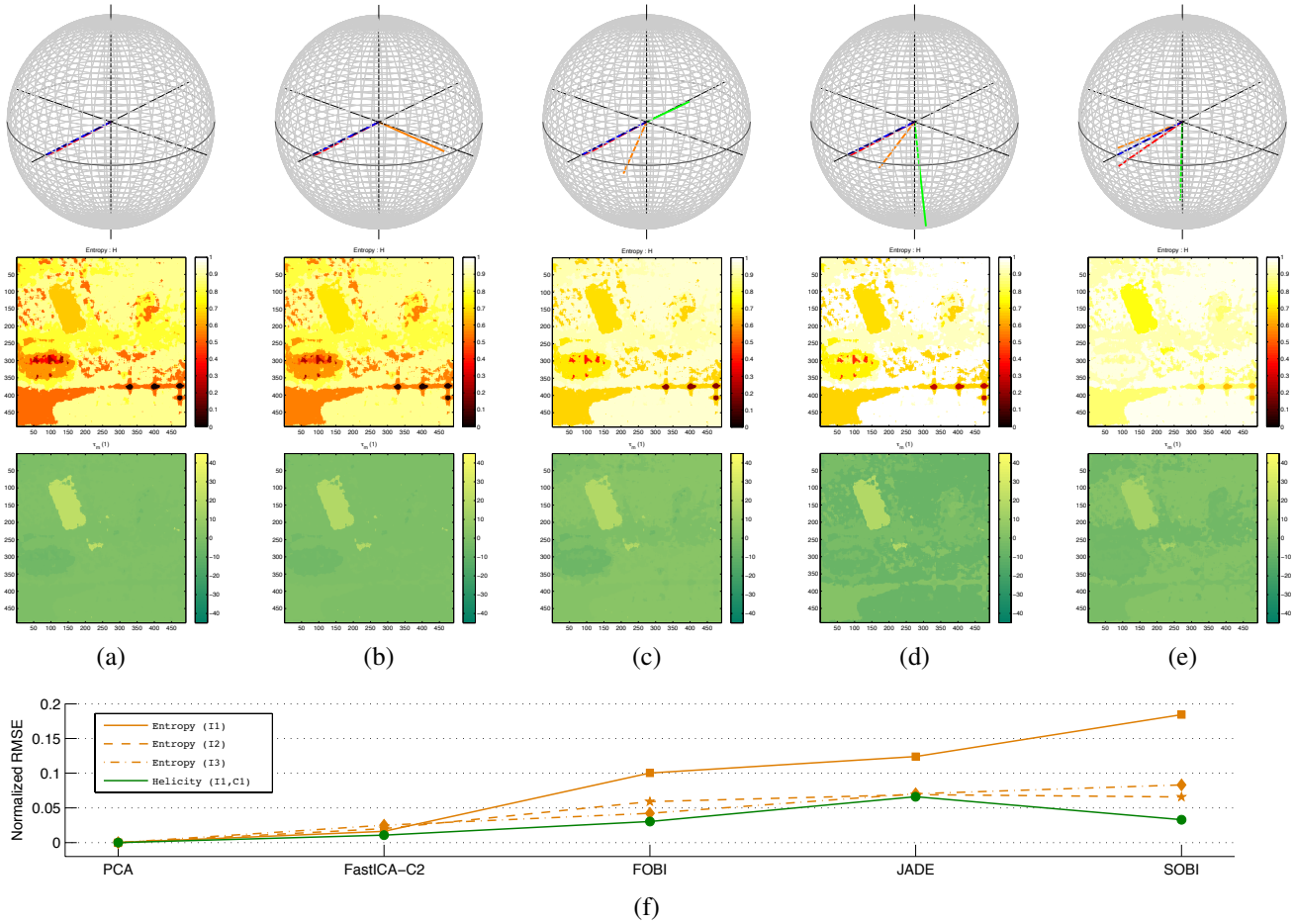

Fig. 1: RAMSES X-band, Brétigny, France. Comparison of different methods based on the Poincaré representation of dominant scatterers (1st row), the entropy (2nd row) and the helicity of the first component (3rd row): (a) PCA, (b) FastICA-C2, (c) FOBI, (d) JADE, (e) SOBI, (f) normalized RMSE with respect to the parameters obtained using PCA.

In [1] the estimation of the independent components is done through the maximization of their Non-Gaussianity, by applying the Complex FastICA algorithm [6]. The comparison between different criteria [1] resulted in choosing the *log* function as the most suitable non-linearity. In this article, two tensorial methods (FOBI, JADE) and one second-order method (SOBI) are applied in the second step and their performances analysed with respect to the same gauges as in [1].

Forth-Order Blind Identification (FOBI) is one of the simplest ICA methods [8]. The independent backscattering mechanisms are derived as eigenvectors of the kurtosis matrix, estimated using whitened set of target vectors ($\tilde{\mathbf{k}}_c$):

$$\mathcal{K}_{\mathbf{I}}(\tilde{\mathbf{k}}) = \mathbb{E}\left[(\tilde{\mathbf{k}}^H\mathbf{I}\tilde{\mathbf{k}})\tilde{\mathbf{k}}\tilde{\mathbf{k}}^H\right] - 2\mathbf{I} - \mathrm{tr}(\mathbf{I})\mathbf{I} = \mathbb{E}\left[|\tilde{\mathbf{k}}|^2\tilde{\mathbf{k}}\tilde{\mathbf{k}}^H\right] - (n+2)\mathbf{I} \quad (1)$$

The most notable drawback of this method would be the condition that all the sources must have quite distant kurtosis values, implicating the failure in case of having several mechanisms characterized with the same distribution.

Joint Approximate Diagonalization of Eigenmatrices (JADE) is a generalization of FOBI [9]. By considering covariance matrix to be a second order cumulant tensor, the kurtosis matrix (Eq. 1) can be considered as a fourth order cumulant tensor of the identity matrix ($\mathcal{K}_{\mathbf{I}} = \mathbf{F}(\mathbf{I})$). Replacing the identity matrix with a set of tuning matrices (eigenmatrices of the cumulant tensor:$\{\mathbf{M_1}, ...\mathbf{M_p}\}$) results in a set of cumulants $\{\mathcal{K}_{\mathbf{M}1}, ...\mathcal{K}_{\mathbf{M}p}\}$. The whitened de-mixing matrix $\tilde{\mathbf{D}}$ is estimated by jointly diagonalizing these matrices, which reduces to the maximization problem:

$$\max_{\tilde{\mathbf{D}}} \mathcal{J}(\tilde{\mathbf{D}}) = \max_{\tilde{\mathbf{D}}} \sum_{i=1}^{p} ||\mathrm{diag}\left(\tilde{\mathbf{D}}\mathcal{K}_{\mathbf{M}p}\tilde{\mathbf{D}}^H\right)||^2 \quad (2)$$

where $||\mathrm{diag}(.)||^2$ is the squared ℓ_2 norm of the diagonal. Given that the maximization of the diagonal elements is equivalent to the minimization of the off-diagonal ones, the resulting de-mixing matrix $\tilde{\mathbf{D}}$ jointly diagonalize the set of cumulants. This algorithm overcomes the mentioned drawback of FOBI, but stays limited to low-dimensional problems.

Second-Order Blind Identification (SOBI) estimates mixing matrix by jointly diagonalizing a set of sample covariance matrices of whitened observations [10]. The obser-

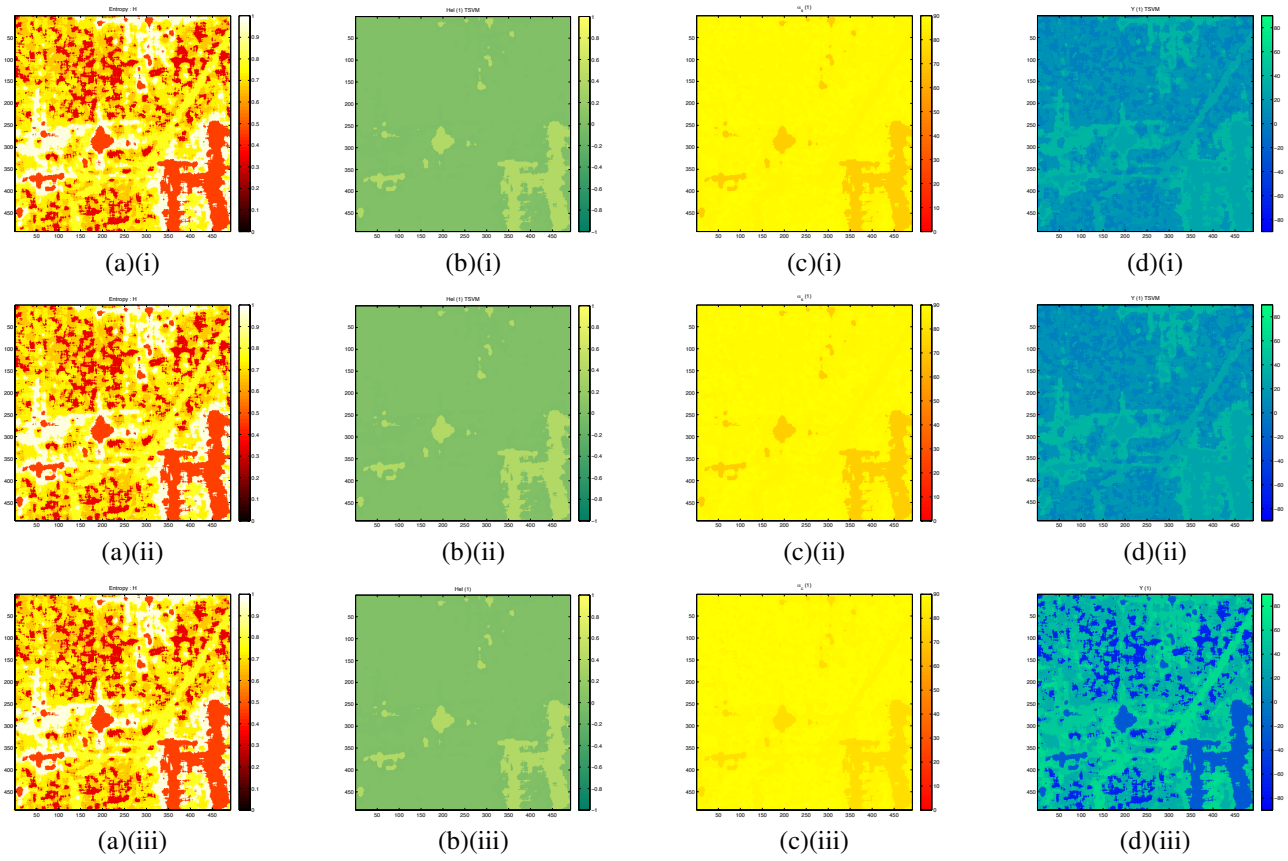

Fig. 2: RAMSES X-band, Toulouse, France. 1st most dominant components in terms of: (a) entropy (H), (b) Hel, (c) α, (d) Υ, for three different cases: (i) no applied rotation in Pauli basis, (ii) applied rotation (15°) in Pauli basis, (iii) circular basis.

vation data are divided into several series (in our case spatial series - subclasses) and each of them is represented by one covariance matrix.

3. INVARIANCE

The invariance with respect to the rotation around of line of sight and to the change of polarization basis represents one of the most appreciated properties of the classical ICTD. In our case, the first property is analysed through the rotation of the observed target vectors, by multiplying them with the orthogonal rotation matrix.

The second property is assessed by applying the proposed ICTD on the data projected on circular polarization basis. The estimated components are parametrized using CPSV parameters: helicity (Hel) and the angles α_c and Υ [11]. The comparison with the decomposition running in the Pauli basis is possible due to the fact that the appropriate counterparts of these CPSV parameters can be derived from the estimated TSVM parameters: $\alpha_c = \alpha_s$ and $\Upsilon = (\pi/2 - \Phi_{\alpha_s})/4$ if $\tau_m = 0$, while:

$$\text{Hel} = \frac{\cos 2\gamma_H \sin 2\tau_m}{\cos^4 \gamma_H \left(1 + tan^4 \gamma_H\right)}. \quad (3)$$

4. RESULTS AND DISCUSSION

Firstly, we have applied the ICA based method on the RAMSES POLSAR X-band image, acquired over Brétigny in France, in order to compare performances obtained using several different ICA algorithms. The criteria for comparison are: the estimation of the entropy and the helicity of the first most dominant component with the ones obtained with PCA and the identification of trihedral in the class corresponding to corner reflectors placed for the purpose of calibration.

As it can be seen in Fig. 1, the initial choice [1], complex non-circular FastICA using logarithmic non-linearity (C2) [6], appears to be the best one with respect to the chosen criteria. Both the entropy and the first component differ significantly in case of applying other ICA algorithms. As well, as we move away from the referent entropy estimation, the second most dominant component seems to converge toward trihedral, implying poor decomposing performances.

RAMSES X-band image acquired over Toulouse in France was used in analysing robustness with respect to the rotation around the line of sight (Fig. 2b) and to the change of polarization basis (Fig. 2c). In both cases we observe the complete (Hel) or the approximate (α) matching of the

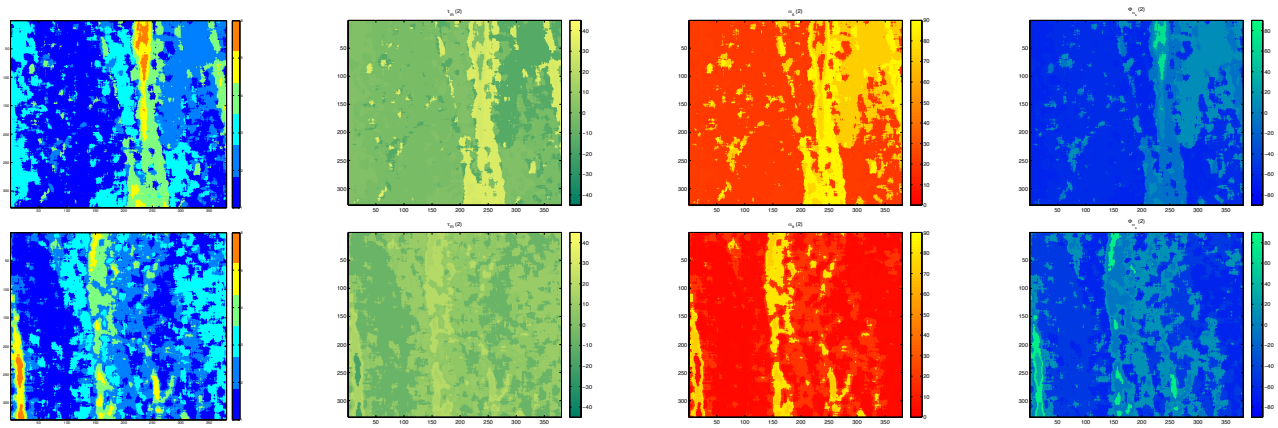

(a) (b) (c) (d)

Fig. 3: ALOS L-band, Chamonix, Mont Blanc, France. (a) classification, (b) helicity (τ_m) of the 2nd component (FastICA-C2), (c) symmetric scattering magnitude (α_s) of the 2nd component (FastICA-C2), (d) symmetric scattering phase (Φ_{α_s}) of the 2nd component (FastICA-C2).

parameters characterizing the estimated components in two considered basis, which effectively demonstrate the invariance i.e. robustness. The differences in case of angle Υ are not affecting this assessment, given that the validity of this parameter happens to be strongly conditioned by the values of helicity and angle α. Namely, we should expect the correspondence only in the case of symmetric target ($\tau_m = 0$), characterized by α which does not converge neither to 0, nor to $\pi/2$.

Image/Class	Class description	$\tau_m[^\circ]$	$\alpha_s[^\circ]$	$\Phi_{\alpha_s}[^\circ]$
I/1	bare ground	**-2.4214**	20.3308	-58.2046
I/2	wet snow	**-14.8296**	72.5023	8.8705
II/1	wet snow	**-7.7216**	3.4504	-48.0882
II/2	dry snow	**6.5860**	18.4891	12.1675
II/3	dry snow	**9.3047**	5.4987	-62.8036

Table 1: ALOS L-band, Chamonix, Mont Blanc, France: roll-invariant parameters of the 2nd dominant component for the labelled classes.

By applying the method based on the FastICA-C2 algorithm on two ALOS POLSAR L-band images, we have noticed an interesting potential information, emerging from the second most dominant component. Namely, using helicity we are able to discriminate between the bare ground, the dry and the wet snow, which doesn't appear as possible neither with the PCA counterpart, neither with other ICA algorithms.

5. CONCLUSION

In this paper, we additionally challenged the form of the ICA based ICDT proposed in [1], by analysing the performances obtained with some different ICA algorithms. However, the initial choice, with respect to the adopted criteria, seems to be the best one. We demonstrated the invariance with respect to both the rotation around the line of sight and the change of polarization basis. As well, we anticipated the utility of the second most dominant component in discriminating between different distributed targets.

6. REFERENCES

[1] N. Besic, G. Vasile, J. Chanussot, S. Stankovic, D. Boldo, and G. d'Urso, "Independent component analysis within polarimetric incoherent target decomposition," in *Proc. IGARSS*, Melbourne, AUS, 2013, pp. 4158–4161.

[2] S. R. Cloude and E. Pottier, "A review of target decomposition theorems in radar polarimetry," vol. 34, no. 2, pp. 498–518, 1996.

[3] R. Touzi, "Target scattering decomposition in terms of roll-invariant target properties," vol. 45, no. 1, pp. 73–84, 2007.

[4] G. Vasile, J. P. Ovarlez, F. Pascal, and C. Tison, "Coherency matrix estimation of heterogeneous clutter in high-resolution polarimetric sar images," vol. 48, no. 4, pp. 1809–1826, 2010.

[5] N. Besic, G. Vasile, J. Chanussot, and S. Stankovic, "Poincare sphere representation of independent scattering sources: application on distributed targets," in *ESA SP-713 - POLinSAR 2013*, Frascati, IT, 2013.

[6] M. Novey and T. Adali, "On extending the complex fastica algorithm to noncircular sources," *IEEE Trans. Signal Processing*, vol. 56, no. 5, pp. 2148–2154, 2008.

[7] A. Hyvarinen, J. Karhunen, and E. Oja, *Independent Component Analysis*, John Wiley and Sons, Inc., New York, NY, USA, 2001.

[8] Jean-François Cardoso, "Source separation using higher-order moments," in *Proc. ICASSP*, Glasgow, May 1989, pp. 2109–2112.

[9] Jean-François Cardoso and Antoine Souloumiac, "Blind beamforming for non Gaussian signals," *IEE Proceedings-F*, vol. 140, no. 6, pp. 362–370, Dec. 1993.

[10] A. Belouchrani, K. Abed Meraim, J.-F. Cardoso, and E. Moulines, "A blind source separation technique based on second order statistics," *IEEE Trans. on Signal Processing*, vol. 45, no. 2, pp. 434–444, 1997.

[11] R. Paladini, L. Ferro-Famil, E. Pottier, M. Mortorella, F. Berizzi, and E. Dalle Mese, "Lossless and sufficient orientation invariant decomposition of random reciprocal target," vol. 50, no. 9, pp. 3487–3501, 2012.

[12] P. Formont, F. Pascal, G. Vasile, J.-P. Ovarlez, and L. Ferro-Famil, "Statistical classification for heterogeneous polarimetric sar images," *IEEE Journal of Selected Topics in Signal Processing*, vol. 5, no. 3, pp. 398–407, 2011.